

**Low elevation transmission measurements at EOPACE;
Part III: Scintillation effects**

Arie de Jong, Gerrit de Leeuw

TNO Physics and Electronics Laboratory
PO Box 96864, 2509 JG The Hague, The Netherlands
Tel: +31-70-3740456 Fax: +31-70-3280961 E-mail: deJong@fel.tno.nl

ABSTRACT

This paper concerns the effect of scintillation on the detection range of infrared sensors, where frame rate appears to play an important role. During EOPACE scintillation measurements were carried out over the Monterey and San Diego Bay. For this purpose 2 kinds of sources were used, either a source, modulated with 1000 Hz, or a DC searchlight source. The detector was a silicon detector with a narrow bandfilter around 0.85 μm . The results show that scintillation is always present, even when locally the air to sea temperature difference (ASTD) is close to zero. This indicates that large ASTD variations may occur along the measurement path. The magnitude of the scintillation agrees reasonably well with the theory. This means a big advantage for high frame rate sensors in comparison with low frame rate sensors for detection of point targets at low elevation.

Keywords: transmission, turbulence, scintillation, atmosphere, boundary layer, EOPACE, infrared, IRST, point target detection.

1. INTRODUCTION

One of the contributions of TNO-FEL at EOPACE was the setup of a transmissometer at low elevation over water. Because of the length of the measurement path (more than 15 km) and the fact that the line of sight was close to grazing the water surface, the location was found to be of interest to the Royal Netherlands Navy. Such paths are likely to occur in the detection process of sea skimming targets with IR sensors. Coastal environments tend to show serious deviations in propagation characteristics of the atmosphere. This was for example observed in the North Sea coastal area during MAPTIP¹, a trial organized by NATO Research Study Group 8, but also in a national experiment over water between Scheveningen and MPN (a platform in the North Sea)^{2,3}. The deviations, mainly due to atmospheric inhomogeneities and layering, have a considerable impact on range prediction models. The US Westcoast is another area where anomalies in propagation can be expected due to the relatively cold water and hot desert in daytime and colder desert at night. The EOPACE campaign, with various international contributions guaranteed a high degree of support measurements, reason for the Netherlands to participate.

The transmissometer, set up by TNO-FEL, was basically the same as that used in 1976, for propagation measurements over an 18 km path between the TNO tower and MPN. The system operates in the 3-5 μm or 8-14 μm spectral band. In addition 3-5 μm imagery was made with a 3-5 μm Focal Plane Array from Cincinnati. Finally scintillation measurements were made with a Near IR (0.85 μm) transmission link, close to the IR lines of sight. A detailed description is given in a preliminary report⁵.

This paper deals with the results of the scintillation measurements. First a crude impression will be given of the impact of scintillation on the detection range of IR sensors for long range point targets. Then the measurement setup will be described in more detail as well as the method of analysis. Data will be presented for both the Monterey and San Diego measurement locations under various conditions. The results will be compared with expected scintillation values, based on ASTD and CNSQ (C_N^2) measurements.

2. IMPACT OF SCINTILLATION ON DETECTION RANGE

The detection range for an IR sensor is directly related to the irradiance level, i.e. the contrast of the point target ΔW and its background at the entrance pupil of the sensor. The irradiance level $I_i(R)$ for a certain frame number i and range R is approximately given by:

$$I_i(R) = \frac{\exp(-\sigma R) \cdot M_i(R)}{R^2} \cdot \Delta W \quad (\Delta W \text{ in } W / \text{ster}) \quad (1)$$

where the atmospheric extinction is approximated by the exponential law $\exp(-\sigma R)$ with σ the total extinction coefficient. This approximation is valid in certain limited spectral bands (eg. 3.7-4.1 μm and 8.5-11 μm). $M_i(R)$ is a modulation function, which rapidly fluctuates, similar to the scintillation in intensity for point sources at long ranges. $M_i(R)$ is referred to as the scintillation function. The irradiance $I_i(R)$ produces a signal in the sensor such that the signal is marked as a candidate detection when a certain signal threshold is passed. The location of this candidate is noted and the next frame is checked for another threshold crossing at the same location. If this happens 3 out of 4 or 4 out of 5 frames, this candidate detection becomes a real detection (confirmed track).

An example of the behaviour of $M_i(R)$ is shown in Figure 1. The possible values of the function M_i increase with range. The curve in Figure 1 has been determined experimentally, but the behaviour corresponds with model predictions such as IR-Tool 6, or the bulk model of Kunz 7. Because of the rather high frequencies in the scintillation spectrum the signal peaks in the image frames vary with tens of Hz. This means that for a frame rate of 1 Hz, the peaks in two consecutive frames are completely uncorrelated.

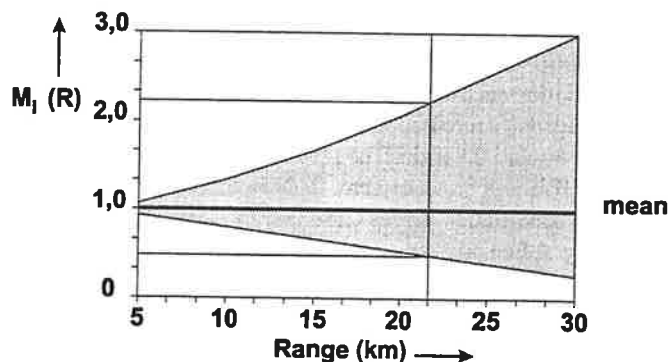


Figure 1. Behaviour of scintillation function $M_i(R)$.

For higher frame rates (eg. 50 Hz), almost always a high peak is observed in at least one of the 50 frames, recorded during 1 second (see also Kunz 3). This leads to the conclusion that the impact of scintillation on detection range for low frame rate sensors can be negative and for high frame rate sensors positive, as illustrated in the following example. Consider two hypothetical sets of sensors, with the same detector array and optics, but with different frame rates, as specified in Table 1.

Table 1. Specifications of hypothetical sensor sets.

	Set 1	Set 2
spectral band	3.6-4.1 μm	3.6-4.1 μm
pupil diameter	180 mm	180 mm
detector array	180 el. Stagg.	180 el. Stagg.
field of view	25(V) \times 75(H) mrad	25(V) \times 75(H) mrad
frame rate	1 Hz	50 Hz
NEI per frame	$5 \cdot 10^{-15} \text{ W/cm}^2$	$3.5 \cdot 10^{-14} \text{ W/cm}^2$

Both sensor sets have the same number of picture elements per frame, so the noise bandwidths for set 1 and set 2 are 400 Hz and 20 kHz. We assume that set 2 has a poorer scan efficiency but less 1/f noise problems. We also assume that the signal processing behind set 2 will average the pictures and select the highest peak of each 50 frames.

The range performance for both sets, taking into account the implications of Formula (1) and Figure 1 concerning scintillation, is presented in Figure 2. In the calculations, the extinction coefficient σ was assumed to be 0.07 km^{-1} and the signal to noise ratio was 5.

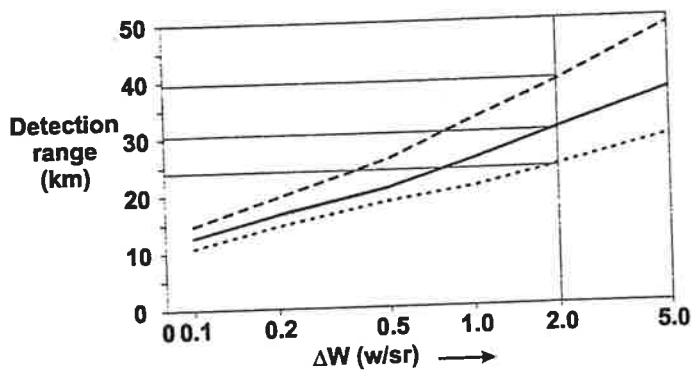


Figure 2. Range performance for high (-----) and low frame (.....) rate sensor as function of target radiant intensity; middle curve (—) no scintillation, both sets; (— · — · —) and (.....) curves with scintillation.

For this example, the scintillation reduces the range performance for the low frame rate set from 30.6 km to 24.2 km for a 2 W/sr target. For the high frame rate set, the range performance increases due to scintillation from 30.6 km to 39.2 km. The operational advantage of an increase in range of 15 km by choosing a faster sensor is evident.

3. MEASUREMENT SETUP, METHODOLOGY

General information on the various instrumentation and setup and their purpose can be found in the testplan⁸. The TNO-FEL transmission locations in the Monterey Bay and San Diego Bay areas are indicated in the maps in Figures 3 and 4.

At the Monterey Site, the sources were mounted at a height of 10 m above mean water level near Moss Landing Pier. The receivers were mounted behind the window of room 1301 of Monterey Plaza Hotel at a height of 16.5 m above mean water level. The distance between source and receiver was 22 km. Unfortunately part of the transmission path (about 1 km) was over the beach at Moss Landing.

At the San Diego site, the sources were mounted on the deck of the Life Guard Station at the Imperial Beach Pier at a height of 9 m above mean water level. The receivers were located in room 146 of the BOQ (building 601) of the Naval Submarine Base. Their height above mean water level was 5.4 m. The distance between source and receiver was 15.1 km. The disadvantage of this site is the frequent crossing of the Line of Sight (LOS) by sailing boats or ships. The IR transmissometry will be discussed in parts I and II^{9,10} of this paper and in reference⁵.

The specifications for the Near IR transmissometer are listed in Table 2. The radiant intensity is given for the spectral response curve, shown in Figure 5.

Table 2. Specifications of Near IR Transmissometer

Parameter	Value
Source: radiant intensity	750 W/sr (peak-peak)
modulation frequency	1000 Hz
divergence	9° (half width)
Receiver: optics diameter	200 mm
optics transmittance	0.9
optics focal length	500 mm
optics receiving area	280 cm ²
detector IFOV	5 mrad
detector responsivity	0.67 · 10 ⁵ V/W
detector noise	6.3 · 10 ⁻⁸ V/√Hz

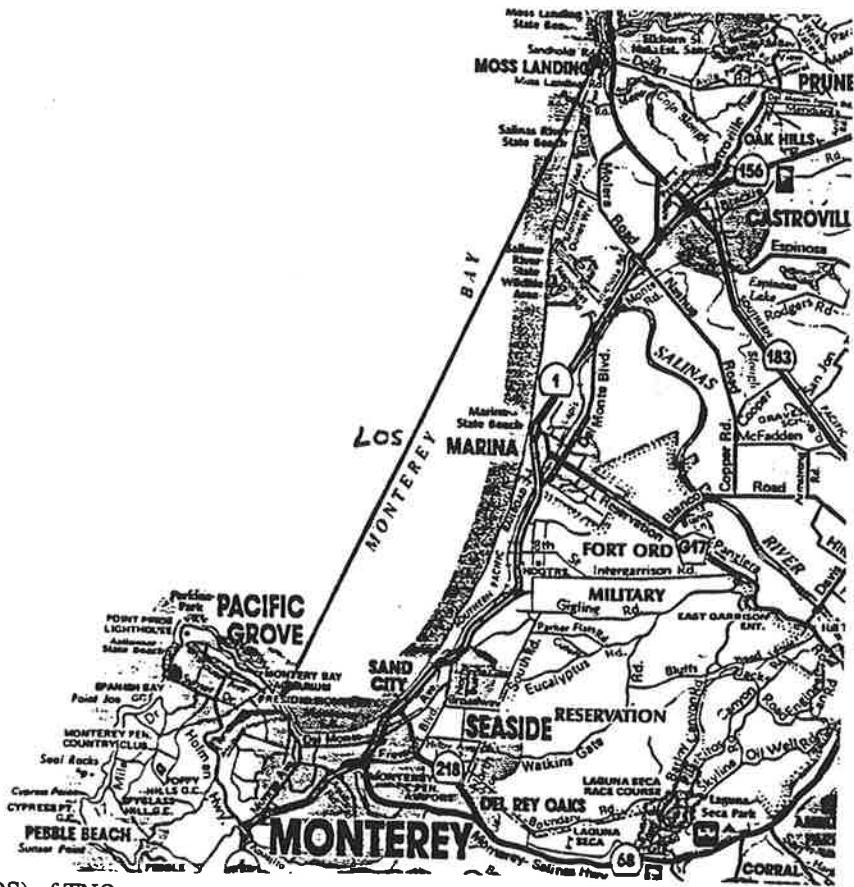


Figure 3. Line of Sight (LOS) of TNO transmissometer at Monterey Bay, 4-15 March 1996.

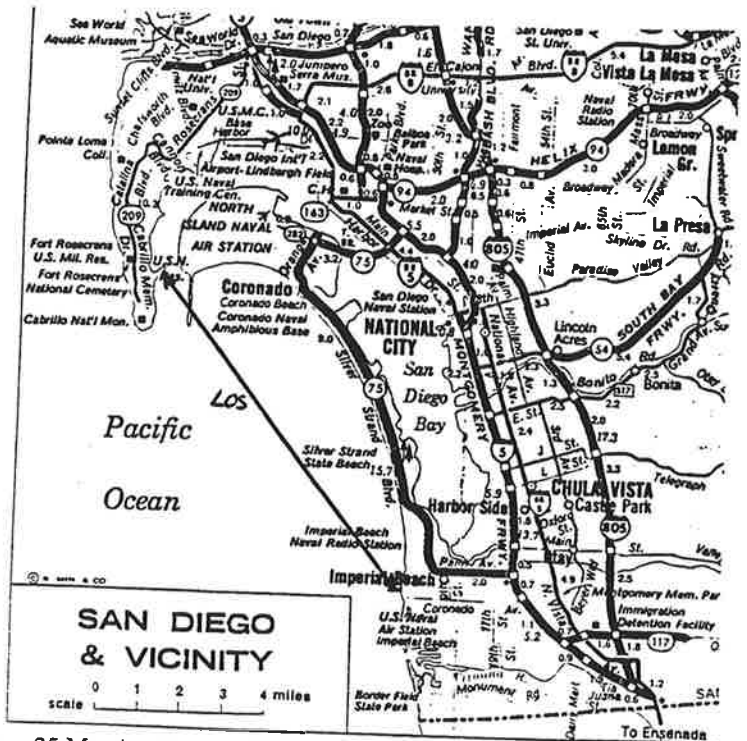


Figure 4. LOS at San Diego Bay, 25 March - 11 April 1996.

The detector signal was amplified by a factor of 2500 by means of a Tektronix 7A22 Scope-unit at 0.2 mV/div setting with frequency limits 0.1-3 kHz. The signal was acquired in 12 bits data acquisition unit with a sampling frequency of 8 kHz. The signal to noise ratio was large enough to obtain the reference signal from the detected signal. In this way, synchronous detection could be achieved in software. The integration time was 10 msec, providing averaging over 10 periods. The atmospheric transmission τ is simply obtained from

$$\tau = 1/462 \cdot (\text{signal in bits}) \text{ or } \tau = 1/932 \cdot (\text{signal in bits}) \quad (2)$$

for the Monterey resp San Diego site, obtained from the laboratory calibration procedure. The signal was recorded during 4 seconds, providing 32000 data samples.

Alternatively the signal of a DC, 2° beam searchlight source was recorded with the same receiver. The radiant intensity in the spectral band of the receiver is about 1 kW/sr. The signal was amplified in the frequency band 0.1 Hz-1 kHz and sampled with 400 Hz in the same AD converter. The signal was recorded in periods of 20 seconds.

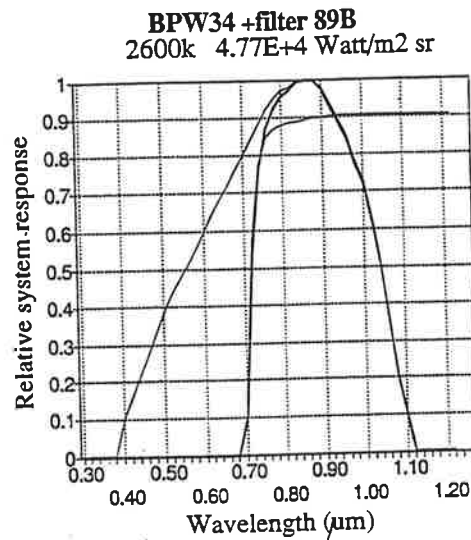


Figure 5. Relative spectral response of Near IR transmissometer.

Analysis of both the AC and DC signal provides direct information on the scintillation in the atmospheric path. The average signal and the statistics of the fluctuations can easily be determined and correlated with simultaneous weather measurements.

In addition to the transmissometry, 3-5 µm imagery was made of a point source, emitting about 200 W/sr in the 3.5-4.7 µm band, where the Cincinnati focal plane array (FPA) cameras were sensitive. One camera (64 × 64 FPA) was in the focus of a 200 mm diameter, 500 mm focal length optical system, providing 0.1 mrad resolution. A second camera (with 160 × 120 elements) was equipped with the standard 50 mm lens, providing 1 mrad resolution. The images were recorded on a double data acquisition unit from Cincinnati IRC-DCB2, in bursts of 128 consecutive frames in 12 bits dynamic range. For the whole set of frames, the sum of all target pixels with respect to the background was calculated, which provides a good impression of the scintillation in a 25 second period.

4. RESULTS

A first impression of the transmission over Monterey Bay over 4 sec time periods is given in Figure 6 for 11 and 12 March around noon. On the 11th the wind was 8 m/sec from land (South). The air and water temperatures were both close to 15°C (see Figure 8). The scintillation over the 22 km path is characterized by (standard deviation STD/average AVG ≈ 0.35) and the average transmission was about 0.08.

Remarkable was that earlier in the morning the windspeed was much smaller while the scintillation was almost as strong as at noon (~0.3). The ASTD was about -2°C at 8 o'clock and probably this thermal unstable situation leads to convective activity producing the observed scintillation. At noon, the stratification was close to neutral, and apparently the mechanical turbulence produced by the wind caused the observed scintillation. When the wind speed decreased in the afternoon, while the ASTD

remained about 0.5°C , the scintillation decreased by more than a factor 2 (< 0.15). Note that the meteo parameters were measured at Moss Landing and may not be representative for the whole transmission path.

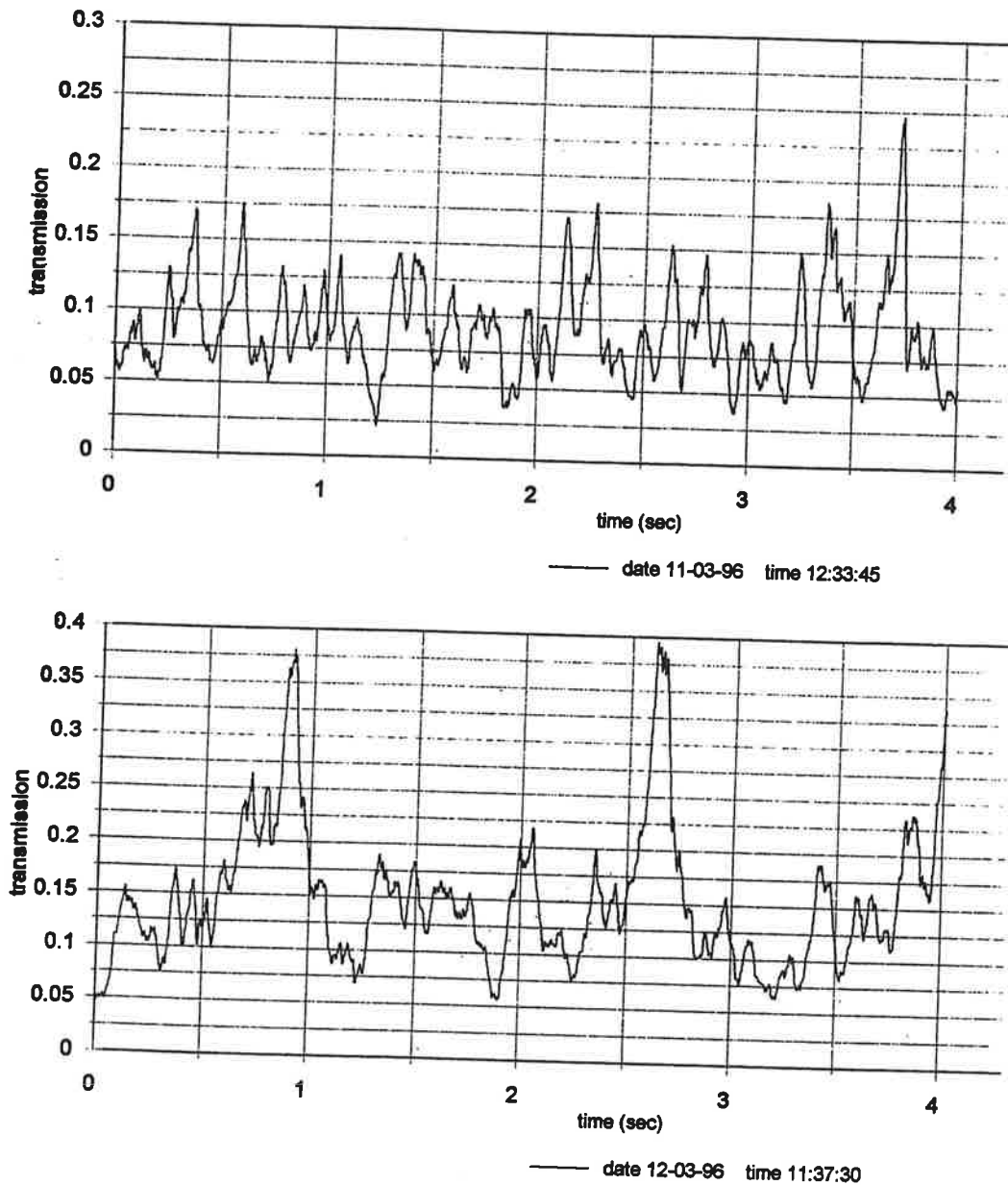


Figure 6. Two examples of $0.85 \mu\text{m}$ transmission data over Monterey Bay (22 km) on 11 and 12 March 1996.

Also remarkable is the magnitude of the fluctuations in transmission. The maximum is about 3 times larger than the average, while the minimum was about 2 times smaller than the average. This behaviour is similar to the prediction based on the $M_i(R)$ curves in Figure 1. Figure 7 shows the variation of STD/AVG with time for the 11th of March, simultaneous with the average transmission. The data for the 12th of March show stronger scintillation with large peaks in the transmission each 1 or 2 seconds. The duration of an outburst was about 0.1 second. From the $10 \mu\text{m}$ transmission plot between 11 and 12 o'clock (not shown here) we conclude that larger scale refraction anomalies were starting to occur, increasing the average $10 \mu\text{m}$ transmission from about 6% to 8% and the $0.85 \mu\text{m}$ average transmission increases to about 0.14%. The anomaly was not expected from the meteo-data at Moss Landing. The difference in temporal behaviour between the 11th and 12th is striking and is expected to have a large effect on the signal processing for IR sensors.

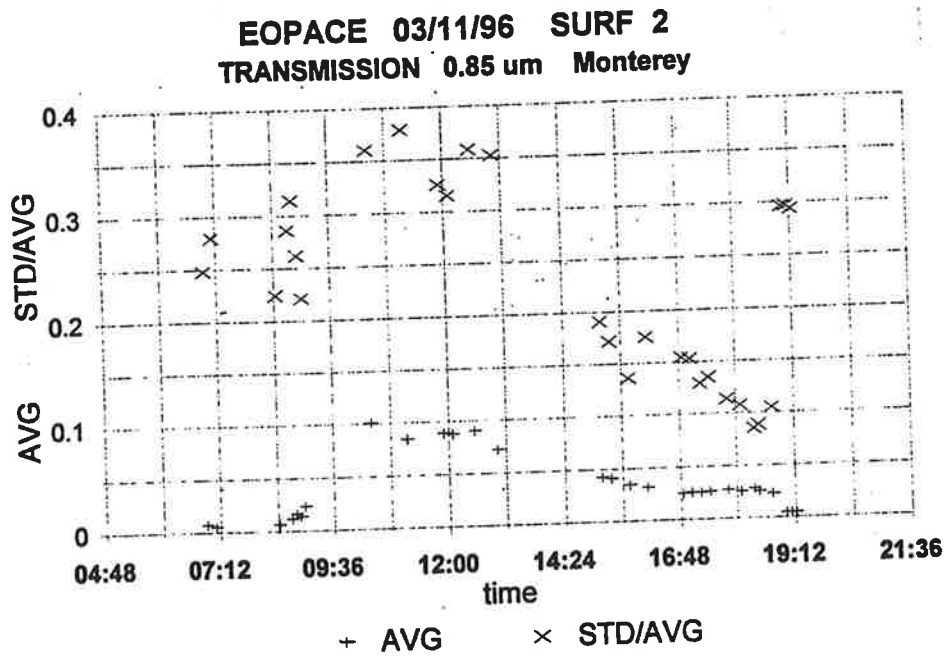


Figure 7. Variation of scintillation with time for 11 March, Monterey.

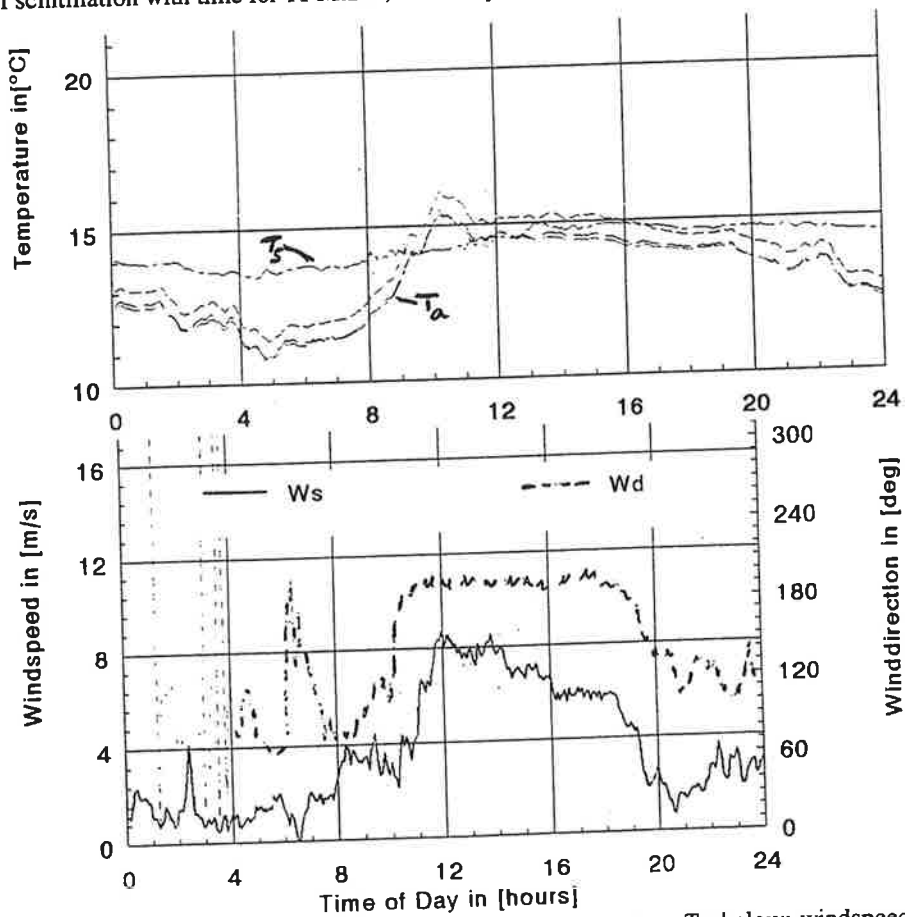


Figure 8. Meteo-data for 11 March; above: air temperature T_a and sea temperature T_s ; below: windspeed and direction at Moss Landing.

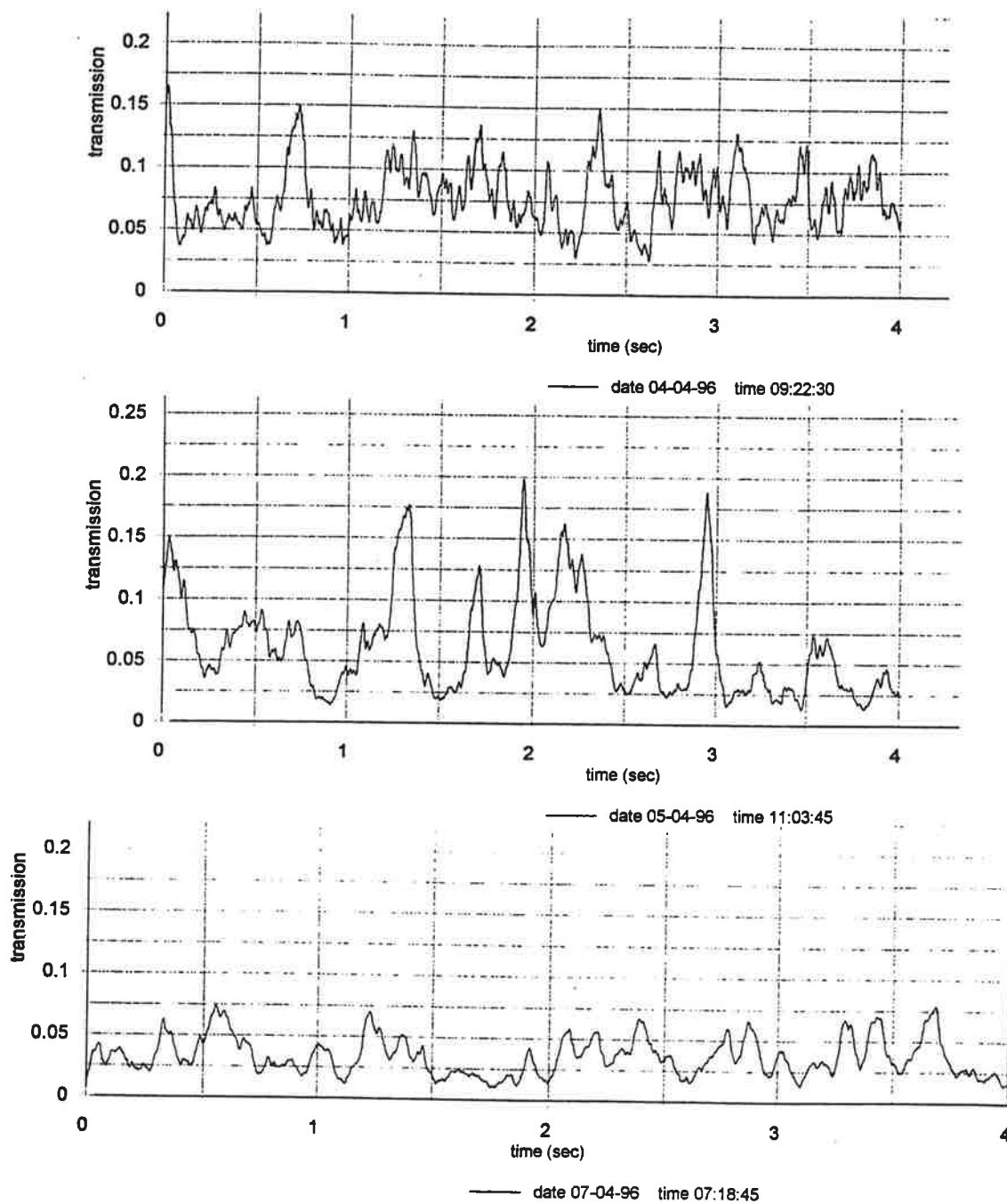


Figure 9. Examples of $0.85 \mu\text{m}$ transmission measurements at San Diego.

Another impression of transmission versus time is given in Figure 9 for the San Diego site for 3 different days, 4, 5 and 7 April. The 4th is a day with rather homogeneous conditions; with fog slowly burning off in the morning. The 5th shows large transmission peaks, similar to those in Figure 6b, due to refraction anomalies starting around 11 o'clock.

The data presented in Figure 9 for 7 April were recorded in an early morning hazy condition, peak-peak fluctuations were still a factor 5, but without the high frequencies.

Figure 10 shows the variation of the scintillation for the 3rd of April from 9.00 in the morning till midnight and refractive index structure coefficient C_N^2 , which is directly responsible for the magnitude of the scintillation.

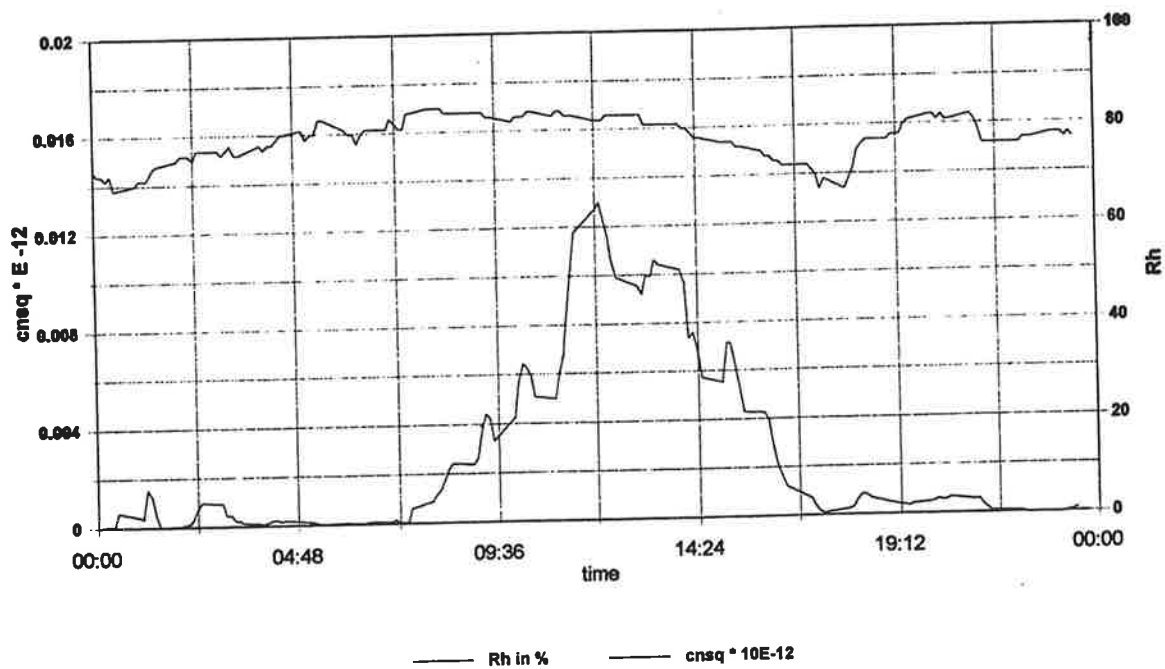
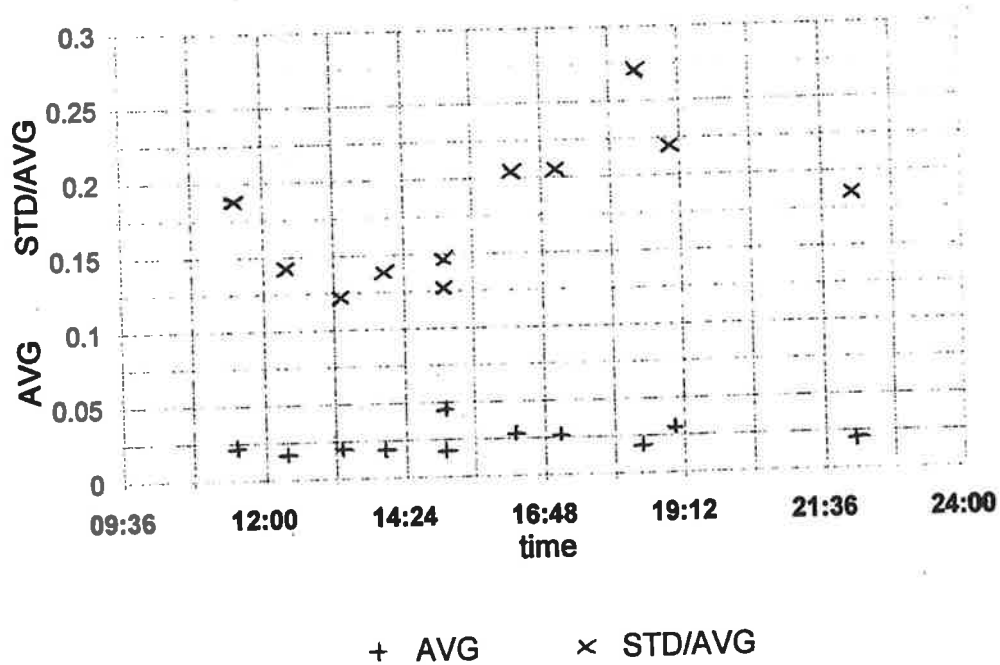


Figure 10. Example of scintillation data for 3 April 1996 San Diego and plot of C_N^2 and relative humidity as function of time.

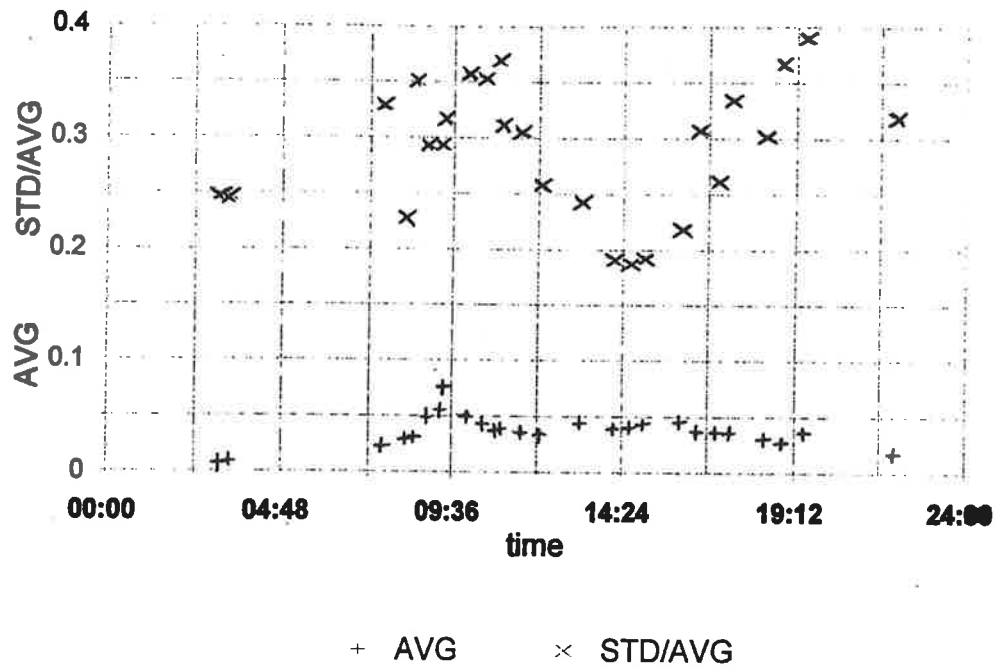


Figure 11. Scintillation data for 4 April at San Diego versus time.

Obviously, there is no correlation between both parameters.

Similarly Figure 11 shows small variations in scintillation for the 4th of April. In the morning with low windspeed (2 m/sec), the scintillation is high (up to 0.35). Around 14.24 the scintillation is less than 0.2 and increasing back again above 0.3 at 19.00. In this case the growth in scintillation corresponds with an increase in windspeed to 5 m/sec. The wind direction changed in the same time from East to West (from land to sea). Air and sea temperatures were about 15°C the whole day.

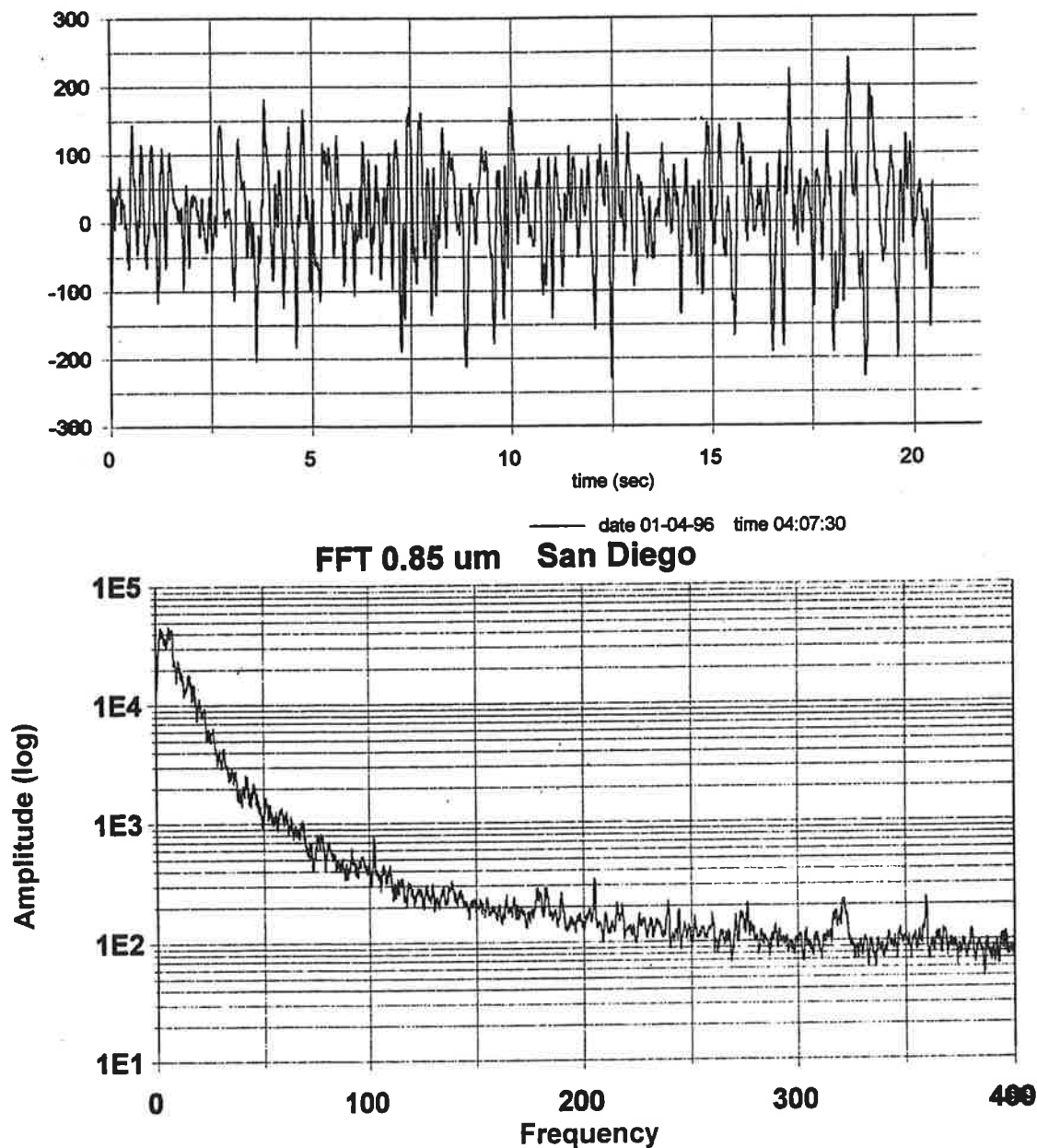


Figure 12. Example of DC source scintillation measurement (above, negative signal corresponds to more light) and fourier spectrum (below) on 1-4-1996.

The following result concerns the "DC" turbulence measurement with the DC source. In Figure 12 data are presented for a 20 second period for the 1st of April at 04.07 in the morning. Fourier transform of the data show the typical behaviour that scintillation intensity decreases with frequency over more than 2 orders of magnitude between 10 and 200 Hz and 1 order of magnitude between 10 Hz and 50 Hz. This means that a frame rate of 50 Hz provides indeed the expected advantage compared to the low frequency (1 Hz) frame rate of standard IRST's.

Figure 13 shows an example of scintillation measurement from 3-5 μm imagery on the 13th of March. The results are similar to those obtained with the scintillation data from the 0.85 μm setup, also shown in Figure 13. It is noted that scintillation measurements with focal plane arrays may contain a certain amount of error due to the undersampling effect of the detector elements. The optical system used however did show a blur, distributing the pointspread function over several elements, reducing greatly the undersampling effect. Apparently the scintillation was rather independent of wavelength for this measurement condition.

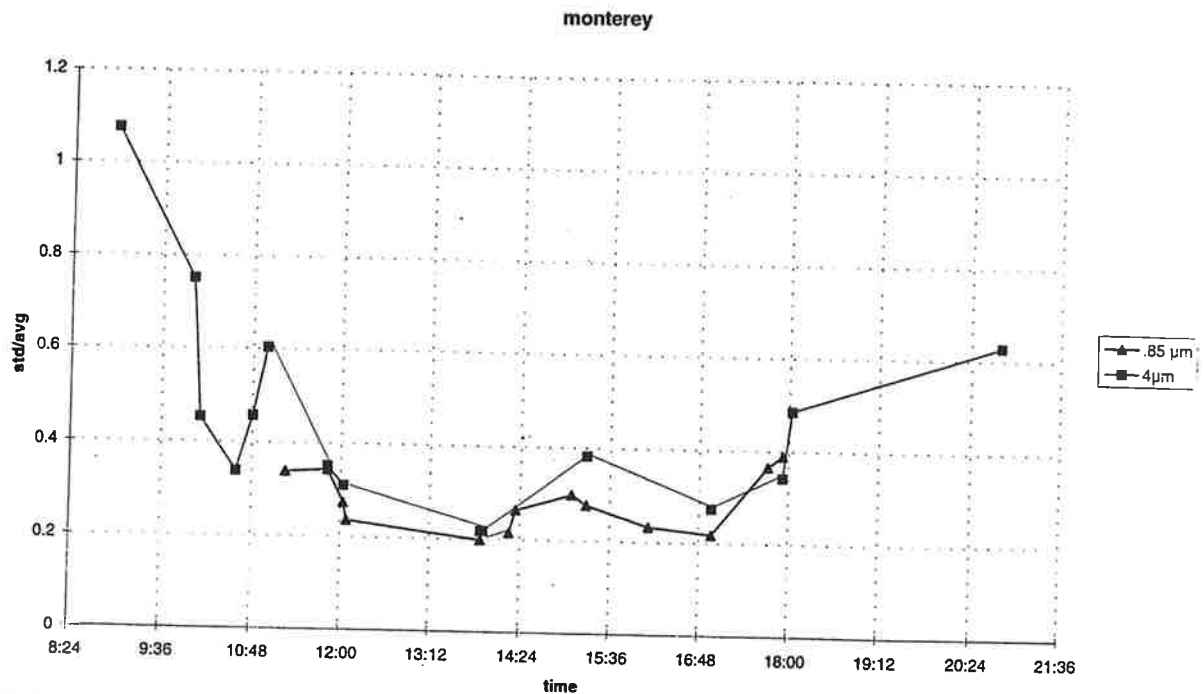


Figure 13. Scintillation data obtained from 3-5 μm imagery for 13 March 1996.

5. DISCUSSION

The scintillation measurements during EOPACE spring 1996 in Monterey and San Diego show that over the 22 and 15 km range the magnitude of the scintillation do not show the variation expected from the weather data. The STD/AVG value between 0.2 and 0.4 (thus the variance between 0.04 and 0.16) stayed within the limits of the weak turbulence (Rytov approximation). The reason for the lack of correlation with the meteo data may be due to the variation of the latter along the path. According to the theory (see for example Beland¹¹) the C_N^2 value should be integrated for all locations at the appropriate height. For a homogeneous path the relation between $(\text{STD}/\text{AVG})^2$ and C_N^2 should be:

$$(\text{STD}/\text{AVG})^2 = 0.496 C_N^2 \left(\frac{2\pi}{\lambda} \right)^{7/6} R^{11/6} \quad (3)$$

where λ is the wavelength (in m) and R the range (in m).

Taking for λ the value $0.85 \cdot 10^{-6}$ and $R = 1.5 \cdot 10^4$, one concludes that C_N^2 should be of the order of $10^{-16} \text{ m}^{-2/3}$. This is much less than predicted from Kunz's bulk model and very much less than the value of 10^{-14} measured at the NPS buoy midway along the path across San Diego Bay.

According to the theory the scintillation should be much less in the infrared, which is not confirmed by the measurements. The scintillation in the IR is still such that high frame rate imaging is preferred because the scintillation effect leads to larger detection ranges.

In conditions of refraction anomalies (due to non linear gradients of the refractive index), transmission peaks can occur during short times (0.15 sec), at a rate of about 1 per second or less.

Several phenomena can provide path inhomogeneities such as high ocean waves and whitecaps, resulting in low level turbulence variations, ocean currents and upwelling resulting in ASTD variations, local wind fields, local variation in water depth (or beach such as at Moss Landing).

It is rather impractical, however, to support the scintillation measurements with a number of weather stations along the path. It should be realized that all these measurements have to be made at various heights between 0.5 and 10 meter. Probably it is in the case of the coastal environment simpler to work with a crude scintillation model based on experiments. As long as insufficient input parameters are available, the models such as the bulk model cannot be validated, using large-path optical transmission. On the other hand, the bulk models can be validated in the meteorological sense for local conditions. It has to be investigated if mid ocean scintillation is smaller than in coastal conditions.

6. CONCLUSIONS AND RECOMMENDATIONS

The scintillation measurements in a coastal environment during EOPACE lead to the following conclusions:

- The variation in the magnitude of the scintillations is more constant than would be expected from weather data.
- The magnitude of the scintillation is less than predicted from the presently available turbulence models.
- The impact of scintillation on IR sensors leads to better performance of the high frame rate sensors and degradation of the performance of low frame rate sensors.
- The atmospheric inhomogeneities along the measurement path required intensive support of model validation measurements by an array of weather stations along the path, which in practice is not feasible.
- It is more practical to set up a crude scintillation model, using very rough input parameters, if the statement is true that scintillation in coastal (and open ocean) conditions stays within rather narrow brackets over the seasons.

It is recommended to continue scintillation measurements over a variety of path lengths in coastal and open ocean conditions.

7. ACKNOWLEDGEMENTS

The efforts of TNO-FEL in EOPACE are supported by the Netherlands Ministry of Defense, project A95KM729 and the US Office of Naval Research, grant N00014-96-1-0581.

For the organization of the EOPACE campaign, NRaD, and in particular Doug Jensen, is acknowledged for splendid arrangements.

In Monterey the NPS personnel, and in particular Ken Davidson and Alf Cooper, are acknowledged for providing supporting data. Authorities at Moss Landing, Imperial Beach and the Naval Submarine Base as well as the personnel from Monterey Plaza Hotel are gratefully acknowledged, in particular the people from the Life Guard Station.

At TNO, Marco Roos is acknowledged for his software support, Ruud Kooyman for improvements in the transmissometer hardware and last but not least Peter Fritz for his great support in the preparation and execution of the trial and for a large part the analysis of the data, and Marcel Moerman for his part in the measurements in Monterey.

8. REFERENCES

1. SPIE Vol 2828; "Image propagation through the atmosphere", Denver, August 1996, Sessions on MAPIP (Marine Aerosol Properties and Thermal Imager Performance)
2. G. de Leeuw et al; "Long-range IR propagation measurements over the North Sea", Proceedings 55th AGARD-EPP specialists' meeting, September 1994, Bremerhaven, Germany
3. G.J. Kunz et al; "Validation of a bulk turbulence model with thermal images of a point source"; SPIE Vol 2828, Denver, August 1996, page 108-116
4. A.N. de Jong; "Long range transmission measurements over sea water", TNO report PHL 1978-08
5. A.N. de Jong et al; "EOPACE Transmission Experiments Spring 1996, Preliminary Results", TNO report FEL-96-A090, October 1996
6. Areté Associates; "IR tool Atmosphere Modelling", Manual Version 2.1.0, ARW-96-303-002-TR, October 1996
7. G.J. Kunz; "A bulk model to predict optical turbulence in a marine surface layer"; TNO report FEL-96-A053
8. D.R. Jensen; "EO Propagation Assessment in Coastal Environments (EOPACE)", Testplan 1995, NRaD-NCCOSC RDTE-DIV San Diego
9. C.R. Zeisse et al.; "Low Elevation Transmission Measurements at EOPACE, part I: Molecular and Aerosol Effects", SPIE Proc Vol 3125, San Diego, July 1997
10. J.L. Forand et al.; "Low Elevation Transmission Measurements at EOPACE, part II: Refraction Effects", SPIE Proc Vol 3125, San Diego, July 1997
11. R.R. Beland; "Propagation through Atmospheric Optical Turbulence", The IR and EO systems Handbook: Vol 2, pp 157-232, SPIE Optical Engineering Press, 1993

PROCEEDINGS OF SPIE



SPIE—The International Society for Optical Engineering

Propagation and Imaging through the Atmosphere

Luc R. Bissonnette
Christopher Dainty
Chairs/Editors

29–31 July 1997
San Diego, California

Sponsored and Published by
SPIE—The International Society for Optical Engineering



Volume 3125

SPIE is an international technical society dedicated to advancing engineering and scientific applications of optical, photonic, imaging, electronic, and optoelectronic technologies.